Stability Control of an Autonomous Vehicle in Overtaking Manoeuvre Using Wheel Slip Control

Armin Norouzi, Ali Barari, Hadi Adibi-Asl

Abstract

Advanced driver assistance systems (ADAS) has been introduced to address driver-related accidents. One of the advantages of ADASs is that they can provide autonomous control and tracking in overtaking manoeuvres via GPS through the designed trajectory. In this study, using adaptive sliding mode control, an integrated longitudinal and lateral control of 4-DOF vehicle's nonlinear dynamic model, in presence of uncertainties, has been proposed. Adaptive control law is utilized for switching gain based on the variations in the sliding surface. Furthermore, a sliding mode control is designed in order to control the longitudinal slip of front wheels. Simulation results show proper tracking for dry roads and acceptable tracking in low adherence roads (wet roads) in overtaking manoeuvres.

Keywords: Autonomous vehicles, Vehicle control, Longitudinal slip control, Sliding mode controller, Adaptive controller

1. Introduction

The contributors to automobile accidents can be categorized into two major groups. first, Inconvenient Environmental Conditions such as poor road condition and poor weather condition. Second, Driver Errors including speeding and unsafe lane change. 94 % of serious crashes are due to human error. Considering more than 35,092 people died in motor vehicle-related crashes in the U.S. in 2015 caused transportation experts have investigated solutions to reduce driver-related errors. Advanced driver assistance systems (ADASs) have been proposed as the best option to address this issue up to now. ADASs can provide autonomous control using three techniques[1]. First, Detection, the controller gains surrounding information via sensors such as LIDAR, RADAR and GPS. Second, Decision Making, the controller designs the desired path based on surrounding information. Third, Action, the controller needs to track the desired path. In this paper, the controller's ability to follow the desired path has been discussed.

Society of Automotive Engineers (SAE) has defined six levels of automation in 2016[2]. Level 0: The human driver does all the driving; Level 1: An advanced driver assistance system (ADAS) on the vehicle can sometimes assist the human driver with either steering or braking/accelerating, but not both simultaneously; Level 2: An advanced driver assistance system (ADAS) on the vehicle can itself actually control both steering and braking/accelerating simultaneously under some circumstances. The human driver must continue to pay full attention (“monitor the driving

environment") at all times and perform the rest of the driving task; Level 3: An Automated Driving System (ADS) on the vehicle can itself perform all aspects of the driving task under some circumstances. In those circumstances, the human driver must be ready to take back control at any time when the ADS requests the human driver to do so. In all other circumstances, the human driver performs the driving task; Level 4: An Automated Driving System (ADS) on the vehicle can itself perform all driving tasks and monitor the driving environment – essentially, do all the driving – in certain circumstances. The human doesn't need to pay attention in those circumstances; Level 5: An Automated Driving System (ADS) on the vehicle can do all the driving in all circumstances. The human occupants are just passengers and need never to be involved in driving. According to National Highway Traffic Safety Administration (NHTSA), we are going through the decade 2016-2025 which consists of Partially Automated Safety Features (e.g., lane keeping assist, adaptive cruise control, traffic jam assist, and self-park technology). It is predicted that the next era, from 2025 on, will consist of Fully Automated Safety Features (Highway Autopilot) [3].

Vehicle active control technology is one of ADASs which plays a key role in vehicle's lateral and yaw stability. Yaw stability enhancement by vehicle active control is the critical requirement for safety of ground vehicles [4]. In order to control yaw rate and lateral stability, a few methods, such as active suspension, active braking and active steering has been proposed. In active suspension, the vehicle's lateral stability is improved by controlling the wheel's work load [5]. In active braking, the lateral stability of vehicle is controlled by Direct Yaw Control (DYC) which adopts differential braking technique [6]. In active steering, the vehicle's lateral stability is improved by controlling the steering angle [6]. Active steering can be classified into three categories as Active Front Steering (AFS), Active Rear Steering (ARS) and Active Four Wheel Steering (4WS). Steering by wire system and mechanical active front steering system are common active front steering (AFS) systems. In steering-by-wire system, there is no mechanical connection between the steering pinion and the steering wheel. In fact, it has been replaced with an electric wire. Mechanical AFS systems utilize motor and planetary gear box to superpose an angle to the steering wheel [7]. These two kinds of AFS can improve vehicle handling and safety by yaw rate tracking control [7]. In the presence of vehicle's external disturbances and model uncertainties, robust control is an integral part of the yaw rate tracking technology of AFS.

Numerous academic researches on the vehicle stability control and active steering control have been conducted. Researchers have proposed different control methods for vehicle active control systems. In [8], a PID controller was used alongside fuzzy logic to control torque for tracking control system. A novel fuzzy logic has been proposed for tracking control systems on low-friction road conditions[9]. In [10], an LQR controller based on the hierarchical control strategy of DYC has been designed in a top-down sequence, which consists of the upper, medium, and lower controllers. An integrated backstepping and sliding mode controller has been used to enhance lateral control of an autonomous grounded vehicle [11]. Model Predictive Control(MPC) has been applied for AFS and DYC integrated control systems to gain more accuracy [12]. Adaptive control has been adopted to improve the performance in the presence of parameter uncertainty [13]. H_∞ controls have been widely applied to the stability control systems [14]. Internal model control (IMC) techniques based on H_∞ optimization are able to satisfy robust stability requirements in the presence of input saturation [15]. Adaptive Sliding Mode Control (ASMC) with fuzzy boundary layer has been adopted to control

vehicle stability for automatic lane change system [16]. Reference [17] proposed a robust path following control which uses the MPC and SMC. However, this control method has been applied to the tire model considering only the side force. Thus, this control method does not deal with longitudinal dynamics.

In this paper, a robust control method utilizing Adaptive Sliding Mode Control (ASMC) for front wheel steering vehicles has been proposed which using a 4-DOF dynamic model considering the variations of velocity. The proposed control enables the vehicle to deal with the coupling of driving force and side force. First, desired trajectory for overtaking manoeuvre will be designed. Next, the 4-DOF vehicle's dynamic model will be introduced. Then, adaptive sliding mode controller for vehicle's longitudinal and lateral motion will be designed. Also, a sliding mode controller for front wheel slip will be proposed. Afterwards, the simulation results will be provided and will be compared to the proposed control in [18]. At the end, final results of this paper will be concluded.

2. Path Planning

We present our desired path for a lane change manoeuvre with acceleration for a front steering vehicle. We assume that there is no other vehicle on the desired path while this overtaking occurs. First, we design a lane change manoeuvre, then, we generalize it to a double lane change.

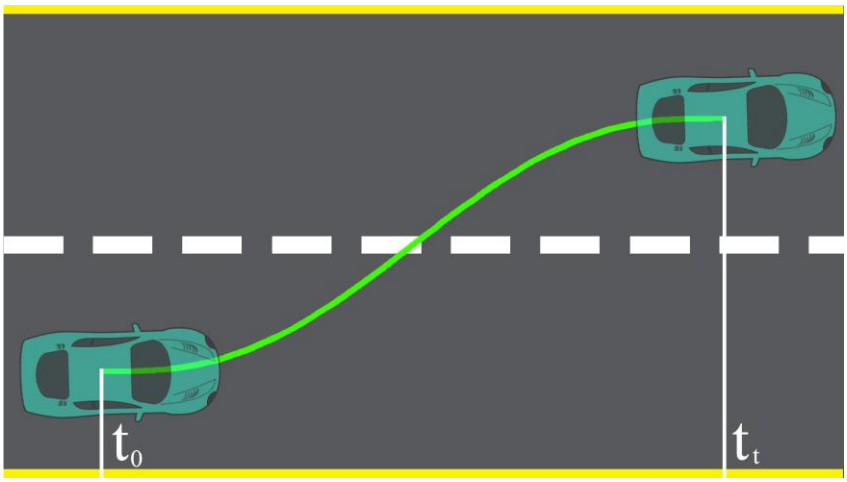

Fig. 1: Lane change manoeuvre for overtaking

Let the S_0 and S_t be state vectors of the vehicle at the start time and end time of each lane change manoeuvre, respectively.

$$\vec{S}_o = (x_o, \dot{x}_o, \ddot{x}_o, y_o, \dot{y}_o, \ddot{y}_o) \quad (1)$$

$$\vec{S}_t = (x_t, \dot{x}_t, \ddot{x}_t, y_t, \dot{y}_t, \ddot{y}_t) \quad (2)$$

Where $x, \dot{x}, \ddot{x}, y, \dot{y}$ and $\ddot{y}$ are the longitudinal displacement, longitudinal velocity, longitudinal acceleration, lateral displacement, lateral velocity and lateral acceleration of the vehicle, respectively.

In order to generate the desired trajectory, a 5th-degree polynomial is utilized in x and y directions [19].

$$x(t) = \sum_0^5 a_i t^i \quad (3)$$

$$y(t) = \sum_0^5 b_i t^i \quad (4)$$

Substituting from (1) and (2) into (3) and (4), the following equations are yielded.

$$[x_0(t) \quad \dot{x}_0(t) \quad \ddot{x}_0(t) \quad x_t(t) \quad \dot{x}_t(t) \quad \ddot{x}_t(t)\,]^T = T_{6\times6}\ A^T \quad (5)$$

$$[y_0(t) \quad \dot{y}_0(t) \quad \ddot{y}_0(t) \quad y_t(t) \quad \dot{y}_t(t) \quad \ddot{y}_t(t)]^T = T_{6\times6}\ B^T \quad (6)$$

Where A, B and T_{6*6} are defined as follows:

$$A^T = [\,a_0 \quad a_1 \quad a_2 \quad a_3 \quad a_4 \quad a_5]^T \quad (7)$$

$$B^T = [\,b_0 \quad b_1 \quad b_2 \quad b_3 \quad b_4 \quad b_5]^T \quad (8)$$

$$T_{6\times6} = \begin{bmatrix} t_0^5 & t_0^4 & t_0^3 & t_0^2 & t_0 & 1 \\ 5t_0^4 & 4t_0^3 & 3t_0^2 & 2t_0 & 1 & 0 \\ 20t_0^3 & 12t_0^2 & 6t_0 & 2 & 0 & 0 \\ t_t^5 & t_t^4 & t_t^3 & t_t^2 & t_t & 1 \\ 5t_t^4 & 4t_t^3 & 3t_t^2 & 2t_t & 1 & 0 \\ 20t_t^3 & 12t_t^2 & 6t_t & 2 & 0 & 0 \end{bmatrix} \quad (9)$$

Substituting from (8) and (9) into (1) and (2) yields:

$$A^T = T_{6\times6}^{-1}\,[x_o, \dot{x}_o, \ddot{x}_o, x_t, \dot{x}_t, \ddot{x}_t]^T \quad (10)$$

$$B^T = T_{6\times6}^{-1}\ [y_o, \dot{y}_o, \ddot{y}_o, y_t, \dot{y}_t, \ddot{y}_t]^T \quad (11)$$

In order to accomplish the first lane change, the vehicle needs to increase its velocity from 10 m/s to 30 m/s with 140 m displacement along the x direction and 3.75 m displacement along the y direction.

$$\vec{S}_o = (x_o, \dot{x}_o, \ddot{x}_o, y_o, \dot{y}_o, \ddot{y}_o) = (0,10,0,0,0,0) \quad (12)$$

$$\vec{S}_t = (x_t, \dot{x}_t, \ddot{x}_t, y_t, \dot{y}_t, \ddot{y}_t) = (140,30,0,3.75,0,0) \quad (13)$$

Then, for the second lane change which completes our desired double lane change (overtaking), we have the following equations:

$$\vec{S}_o = (x_o, \dot{x}_o, \ddot{x}_o, y_o, \dot{y}_o, \ddot{y}_o) = (0,30,0,3.75,0,0) \quad (14)$$

$$\vec{S}_t = (x_t, \dot{x}_t, \ddot{x}_t, y_t, \dot{y}_t, \ddot{y}_t) = (140,25,0,0,0,0) \quad (15)$$

3. Vehicle's Dynamics Model

In this case study, a simplified bicycle model with four-degrees-of-freedom (4-DOF) is used to model vehicle dynamics [20]. The four degrees of freedom are due to the vehicle's lateral position *y*, longitudinal position *x*, the vehicle's yaw angle ψ and front wheels rotationω_w, as shown in Fig. 2.

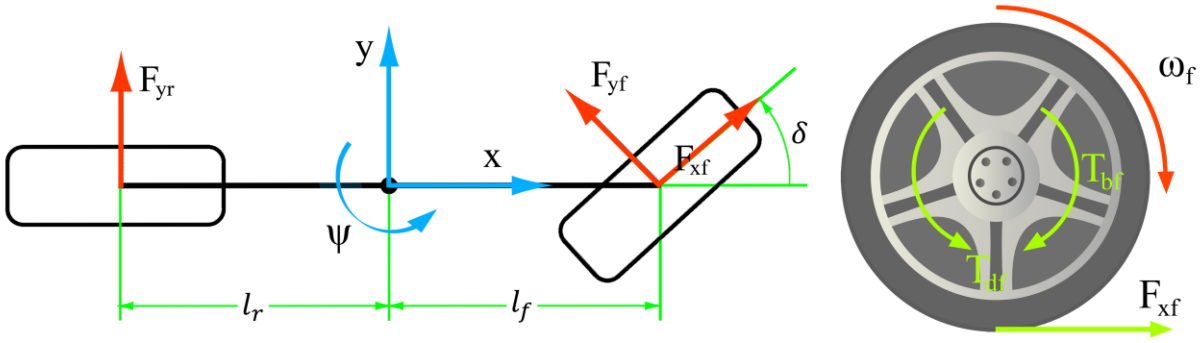

Fig. 2: Four-degree-of-freedom (4-DOF) vehicle-bicycle model.

$$m\ddot{x} = F_{xf}\cos\delta + F_{xr} - F_{yf}\sin\delta - m\dot{\psi}\dot{y} \quad (16)$$

$$m\ddot{y} = F_{yr} + F_{xf}\sin\delta + F_{yf}\cos\delta - m\dot{\psi}\dot{x} \quad (17)$$

$$I_z\ddot{\psi} = l_f F_{xf}\sin\delta + l_f F_{yf}\cos\delta - l_r F_{yr} \quad (18)$$

$$I_w\dot{\omega}_w = T_{df} + T_{bf} - r_{eff}F_{xf} \quad (19)$$

Simulation parameters are provided in Appendix 1.

The lateral slip angle for front and rear wheels can be written as:

$$\alpha_f = \delta - \frac{\dot{y}+l_f\dot{\psi}}{\dot{x}} \quad (20)$$

$$\alpha_r = -\frac{\dot{y}-l_r\dot{\psi}}{\dot{x}} \quad (21)$$

Also, the longitudinal slip ratio for front wheels in accelerating and braking time can be expressed as:

$$\sigma_x = \frac{r_{eff}\omega_\omega - \dot{x}}{\dot{x}} \quad \text{braking} \quad (22)$$

$$\sigma_x = \frac{r_{eff}\omega_\omega - \dot{x}}{r_{eff}\omega_\omega} \quad \text{accelerating} \quad (23)$$

Dugoff's tire model has been chosen for this study [20]. Equations for this model are given by:

$$F_x = C_\sigma \frac{\sigma_x}{1+\sigma_x} f(\lambda) \quad (24)$$

$$F_y = C_\alpha \frac{\tan(\alpha)}{1+\sigma_x} f(\lambda) \quad (25)$$

$$\begin{cases} f(\lambda) = (2-\lambda)\lambda & \lambda < 1 \\ f(\lambda) = 1 & \lambda \geq 1 \end{cases} \quad (26)$$

$$\lambda = \frac{\mu F_z(1+\sigma_x)}{2\left\{(C_\sigma\sigma_x)^2 + (C_\alpha\tan(\alpha))^2\right\}^{\frac{1}{2}}} \quad (27)$$

Furthermore, the following assumptions are considered in this study:

I. The vehicle uses only front wheels to steer.
II. The front wheel steering angle is small, so the equations can be linearized.
III. Accelerating mode is considered.
IV. Lateral load transfer is neglected.

$$F_{yf} = C^*_{\alpha f}\alpha_f \quad (28)$$

$$F_{yr} = C^*_{\alpha r}\alpha_r \quad (29)$$

where C^*_α can be shown as [21]:

$$C^*_{\alpha f} = \mu C_{\alpha f} \quad (30)$$

$$C^*_{\alpha r} = \mu C_{\alpha r} \quad (31)$$

Now, the final equations for designing the controller are obtained as follows:

$$\begin{bmatrix} \ddot{x} \\ \ddot{y} \\ \ddot{\psi} \\ \omega_f \end{bmatrix} = \begin{bmatrix} F_1 \\ F_2 \\ F_3 \\ F_4 \end{bmatrix} + \begin{bmatrix} G_1 & 0 & 0 \\ 0 & G_2 & 0 \\ 0 & G_3 & 0 \\ 0 & 0 & G_4 \end{bmatrix} \begin{bmatrix} F_x \\ \delta \\ T_f \end{bmatrix} \quad (32)$$

$$[\vec{\dot{x}}] = [\vec{F}] + [\vec{G}][\vec{u}] \quad (33)$$

where,

$$F_1 = \dot{\psi}\dot{y}$$

$$F_2 = -\frac{1}{m}\left\{\mu C_{\alpha r}\frac{\dot{y}-l_r\dot{\psi}}{\dot{x}} + \mu C_{\alpha f}\frac{\dot{y}+l_f\dot{\psi}}{\dot{x}}\right\} - \dot{\Psi}\dot{x}$$

$$F_3 = \frac{l_r\mu C_{\alpha r}}{I_z}\left(\frac{\dot{y}-l_r\dot{\psi}}{\dot{x}}\right) - \frac{l_f\mu C_{\alpha f}}{I_z}\left(\frac{\dot{y}+l_f\dot{\psi}}{\dot{x}}\right)$$

$$F_4 = -\frac{r_{eff}}{I_\omega}F_{xf}$$

$$G_1 = \frac{1}{m}$$

$$G_2 = \frac{1}{m}\left(\mu C_{\alpha f} + F_{xf}\right)$$

$$G_3 = \frac{l_f}{I_z}\left(F_{xf} + \mu C_{\alpha f}\right)$$

$$G_4 = \frac{1}{I_\omega}$$

4. Controller Design

4.1. Vehicle's longitudinal and lateral controller design

In this section, an adaptive sliding mode controller (ASMC) with constant boundary layer has been proposed. The adaptive control law updates switching gain based on the variations in the sliding surface. Defining sliding surfaces based on the system errors is the first step in controller design. Next, the adaptive control law is applied. In Appendix 2, by using the definition of Lyapunov function, the controller stability has been proved analytically. As the vehicle model is based on the second order differential equations (n = 2), the sliding surface is selected as follows:

$$\vec{S} = \left(\frac{d}{dt} + \lambda\right)^{n-1}\tilde{x} \quad (34)$$

where,

$$\tilde{x} = \begin{bmatrix} e_x \\ e_y \end{bmatrix} \quad (35)$$

and longitudinal and lateral error can be expressed as: $e_x = \dot{x} - \dot{x}_{ref}$

$$e_x = \dot{x} - \dot{x}_{ref} \quad (36)$$

$$e_y = e_1 + de_2 \tag{37}$$

$$\dot{e}_1 = \dot{y} + \dot{x}e_2 \tag{38}$$

$$e_2 = \psi - \psi_{ref} \tag{39}$$

Which e_1 is the distance of the c.g. of the vehicle from the center line of the lane, e2 is the orientation error of the vehicle with respect to the road and d is the longitudinal distance of the point ahead of the vehicle c.g. at which the sensor measurement is made.

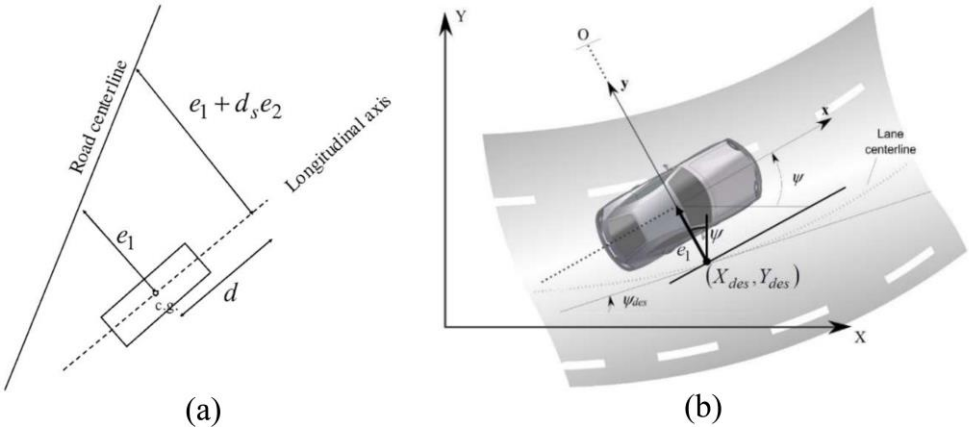

Fig. 3: (a) Look ahead lateral position measurement with respect to road. (b) From body fixed to global coordinates [20]

According to the above equations, the sliding surface is obtained as:

$$\vec{S} = \dot{\tilde{x}} + \lambda\tilde{x} = \begin{bmatrix} \dot{e}_x \\ \dot{e}_1 + d\dot{e}_2 \end{bmatrix} + \begin{bmatrix} \lambda_1 & 0 \\ 0 & \lambda_2 \end{bmatrix} \begin{bmatrix} e_x \\ e_1 + de_2 \end{bmatrix} \tag{40}$$

By differentiating Equation (40), the following equation is obtained.

$$\dot{\vec{S}} = \begin{bmatrix} \ddot{e}_x + \lambda_1\dot{e}_x \\ \ddot{e}_1 + d\ddot{e}_2 + \lambda_2\dot{e}_1 + \lambda_2 d\dot{e}_2 \end{bmatrix} \tag{41}$$

Substituting from (35-38) into (40) yields:

$$\dot{\vec{S}} = \begin{bmatrix} \hat{F}_1 + \hat{C}_1 F_x - \ddot{x}_{ref} + \lambda_1\dot{x} - \lambda_1\dot{x}_{ref} \\ \hat{F}_2 + \hat{C}_2\delta + \left(\hat{F}_1 + \hat{C}_1 F_x\right)e_2 + \dot{x}\dot{e}_2 + d\hat{F}_3 + d\hat{C}_3\delta - d\ddot{\psi}_{ref} + \lambda_2 e_1 + \lambda_2 d\dot{e}_2 \end{bmatrix} \tag{42}$$

According to [22], the best control law for $\tilde{x}$ error is achieved when $\dot{\vec{S}} = 0$.

$$\begin{bmatrix} F_{xeq} \\ \delta_{eq} \end{bmatrix} = -\begin{bmatrix} \frac{1}{\hat{b}_x} & 0 \\ 0 & -\frac{1}{\hat{b}_y} \end{bmatrix} \begin{bmatrix} \hat{F}_x \\ \hat{\delta} \end{bmatrix} \tag{43}$$

where $\hat{\delta}$ andare given by $\hat{F}_x$

$$\hat{F}_x = \hat{F}_1 - \ddot{x}_{ref} + \lambda_1\dot{x} - \lambda_1\dot{x}_{ref} \quad , \quad \hat{b}_x = \hat{G}_1 \tag{44}$$

$$\hat{\delta} = \hat{F}_2 + \hat{F}_1 e_2 + \hat{G}_1 F_x e_2 + \dot{x}\dot{e}_2 + d\hat{F}_3 + \lambda_2\dot{e}_1 + \lambda_2 d\dot{e}_2 - d\ddot{\psi}_{ref}, b_y = \hat{G}_2 + d\hat{G}_3 \tag{45}$$

Based on [22], slip condition is introduced as Equation (46),

$$\frac{1}{2}\frac{\mathrm{d}}{\mathrm{dt}}\vec{S}^2(\mathrm{t}) \le \eta\left|\vec{S}(\mathrm{t})\right| \tag{46}$$

where η is a strictly positive constant [22]. To satisfy this condition, one term is added to F_{xeq} and δ_{eq},

$$\vec{u}_{SMC} = -\begin{bmatrix} \frac{1}{\hat{b}_x} & 0 \\ 0 & -\frac{1}{\hat{b}_y} \end{bmatrix}\begin{bmatrix} \hat{F}_x + k_x\, sign(s_1) \\ \hat{\delta}_1 + k_y\ \ sign(s_1) \end{bmatrix} \tag{47}$$

To establish the sliding condition (46), the range of k is calculated similar to [20] [see Appendix 2]. To avoid chattering, instead of the sign function, a saturated function has been proposed.

$$\mathrm{sat}\left(\frac{\mathrm{s}}{\varphi}\right) = \begin{cases} 1 & \frac{\mathrm{s}}{\phi} > 1 \\ \frac{\mathrm{s}}{\varphi} & -1 < \frac{\mathrm{s}}{\phi} < 1 \\ -1 & \frac{\mathrm{s}}{\phi} < -1 \end{cases} \tag{48}$$

Thus,

$$\vec{u}_{SMC} = \begin{bmatrix} -\frac{1}{b_x}\left(\hat{F}_x + k_x\, sat(s_1/\varphi_1)\right) \\ -\frac{1}{b_y}\left(\hat{\delta}_1 + k_y\ sat(s_1/\varphi_2)\right) \end{bmatrix} \tag{49}$$

In this study, the value of ϕ is considered 0.01.

In this section, an adaptive control law is applied on the sliding mode controller. The adaptive control law has been defined in Equations 50 and 51, where B is the switching gain and presents an estimation of k, as follows [16]:

$$\dot{B}_1 = \gamma_x|S_1(t)| \tag{50}$$

$$\dot{B}_2 = \gamma_y|S_2(t)| \tag{51}$$

Therefore, the adaptive sliding mode control can be obtained.

$$\vec{u}_{ASMC} = \begin{bmatrix} \frac{-\left(\hat{F}_x + B_1\gamma_x sat(S_1/\phi_1)\right)}{\hat{G}_1} \\ \frac{-\left(\hat{\delta} + B_2\gamma_y sat(S_2/\phi_2)\right)}{\hat{G}_2 + d\hat{G}_3} \end{bmatrix} \tag{52}$$

The range of γ_x and γ_y has been discussed in Appendices 3 and 4.

4.2. Front wheel slip controller design

In order to control the longitudinal slip of tire, the sliding mode control has been adopted. Due to ABS's non-linear equations and its uncertainties, the sliding mode control would show acceptable robustness. The system of equations to design the controller is as follows:

$$\dot{\omega}_f = F_4 + G_4 T_f \tag{53}$$

The longitudinal slip ratio for acceleration is written as (54). In order to remove the slip, it has been considered as error, as written in (55) [23].

$$\lambda = \frac{r_{eff}\omega_f - \dot{x}}{r_{eff}\omega_f} \tag{54}$$

$$e_s = \frac{r_{eff}\omega_f - \dot{x}}{r_{eff}\omega_f} - 0 = \lambda \quad (55)$$

The sliding surface can be obtained as:

$$S_s = e_s \quad (56)$$

By differentiating the sliding surface, the following equation is obtained:

$$\dot{S}_s = -\frac{\ddot{x} r_{eff}\omega_f - r_{eff}\dot{\omega}\dot{x}}{{r_{eff}}^2\omega^2} \quad (57)$$

Substituting from (53) into (57) yields:,

$$\dot{S}_s = \frac{r_{eff}\dot{\omega}_f(1-\lambda) - \ddot{x}}{r_{eff}\omega_f} = \frac{(\hat{F}_4 + \hat{G}_4 T_f) r_{eff}(1-\lambda) - \hat{F}_1 - \hat{G}_1 F_x}{r_{eff}\omega_f} \quad (58)$$

According to [22], the best control law is as follows:

$$\dot{\vec{S}} = 0 \quad \Rightarrow \quad T_{feq} = \frac{-1}{\hat{G}_4 r_{eff}(1-\lambda)} \hat{T}_f \,, \qquad \hat{b}_s = \hat{G}_4 r_{eff}(1-\lambda) \quad (59)$$

where,

$$\hat{T}_f = r_{eff}\hat{F}_4(1-\lambda) - \hat{F}_1 - \hat{G}_1 F_x \quad (60)$$

The slip condition is defined as:

$$\frac{1}{2}\frac{\mathrm{d}}{\mathrm{dt}} S_s^2(\mathrm{t}) \leq \eta_s |S_s(\mathrm{t})| \quad (61)$$

In order to satisfy this condition, one term has been added to T_{feq} ,

$$T_{fsmc} = -\frac{1}{\hat{G}_4 r_{eff}(1-\lambda)} \left(\hat{T}_f - k_s sat\left(\frac{S_s}{\phi_s}\right) \right) \quad (62)$$

where k_s and $\bar{F}_s$ [22],

$$k_s \geq \bar{F}_s + \eta_s \quad (63)$$

$$\bar{F}_s = r_{eff}\bar{F}_4(1-\lambda) - \bar{F}_1 - \bar{G}_1 F_x \quad (64)$$

Finally, the block diagram of the controller has been designed by combining the longitudinal, lateral, and tire slip controller, as shown in Fig. 4.

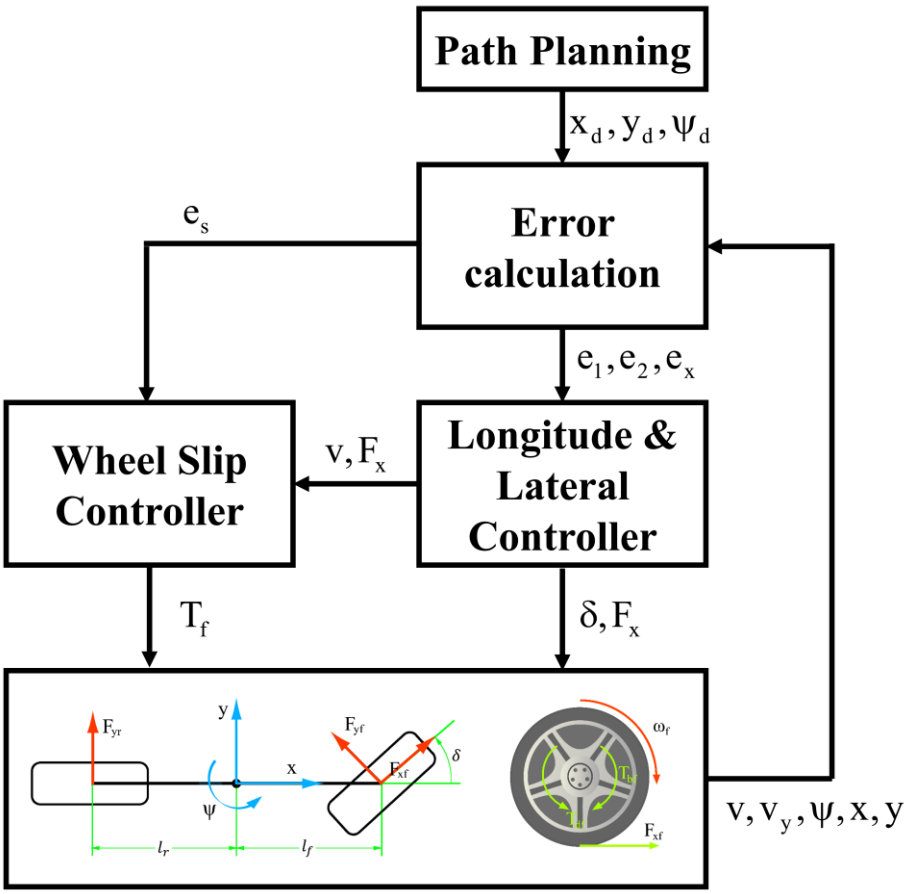

Fig. 4: The block diagram for the proposed control in this study

5. Discussion and Results

In this study, the results of the proposed controller has been compared to that of the controller in [18]. They have designed a path-following steering controller using MPC with adaptive preview time (APT) for automated LCS. A bicycle model has been employed to design the prediction model. They have used a ramp sinusoidal function to generate the desired lane change path. The optimal steering angle command for the LCS has been determined by minimizing the cost function which consists of the lateral displacement errors between the target path and the predicted path, and the steering angles within the prediction horizon in [18].

In [18], the input function for lane change manoeuvre is given by:

$$X = v_s t, Y = w\left[\frac{t}{T_{tot}} - \frac{1}{2\pi}\sin(\frac{2\pi}{T_{tot}}t)\right] \quad (65)$$

In the current research, the same input as in [18] has been used for the proposed controller and the results have been compared with that of [18].

According to Fig. 5, the proposed controller has been able to track the path with a higher accuracy than the proposed control in [18].

As shown in Fig. 6, the controller response for double lane change (overtaking) is appropriate. The maximum error for longitudinal control is 0.2. Also, the longitudinal control is able to generate the desired velocities, from 10 m/s to 30 m/s in the first lane change, then to 25 m/s in the second lane change. According to the sliding surface, the adaptive control has been able to estimate the proper value for switching surface, the value of which is constant for each lane change. Also, the sliding mode control is able to generate the appropriate torque for wheels, which removes the longitudinal slip for front wheels.

According to Fig. 7, the controller appropriately tracks the path on low adherence roads (wet roads) with no chattering. While the tracking is not exact, the controller is robust with uncertainties (small acceptable errors) based on road condition. Due to the appropriate tracking of the velocity and lateral error, the delay in yaw angle tracking has less effect on the system. According to Fig. 7, the adaptive coefficient has been reached in less than 1 second. By starting the lane change manoeuvre, the adaptive coefficient has increased to 4.2 in less than 2 seconds. Excepting for dry road conditions, the higher values of the adaptive coefficient shows higher energy consumption of the system to deal with uncertainties. Based on the steering angle diagram, because the input is a continuous curve, the controller input is applicable to the experimental environment. Tire angular velocity diagram shows proper tracking in terms of v/r_{eff}. The longitudinal slip controller has been designed to optimize wheel's torque in order to avoid tire slip. Although reaching to this level of tracking accuracy is far away in real conditions, the controller showed proper results in the simulation environment.

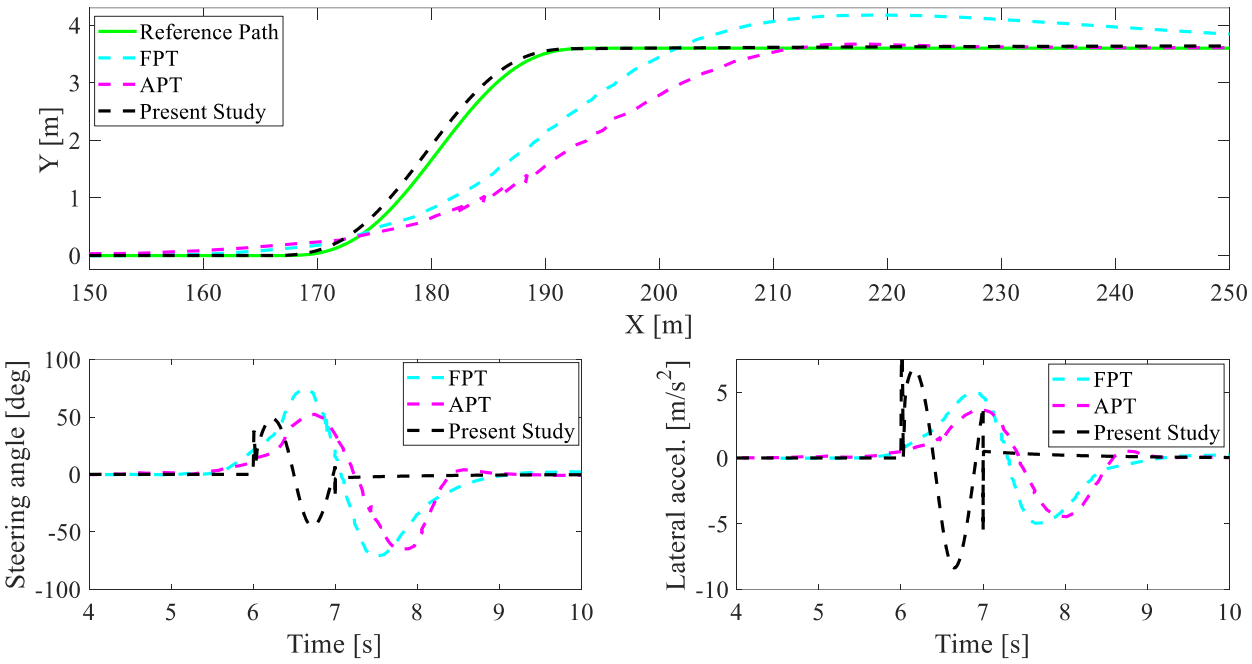

Fig. 5: Comparing the proposed controller with the controller in [18]

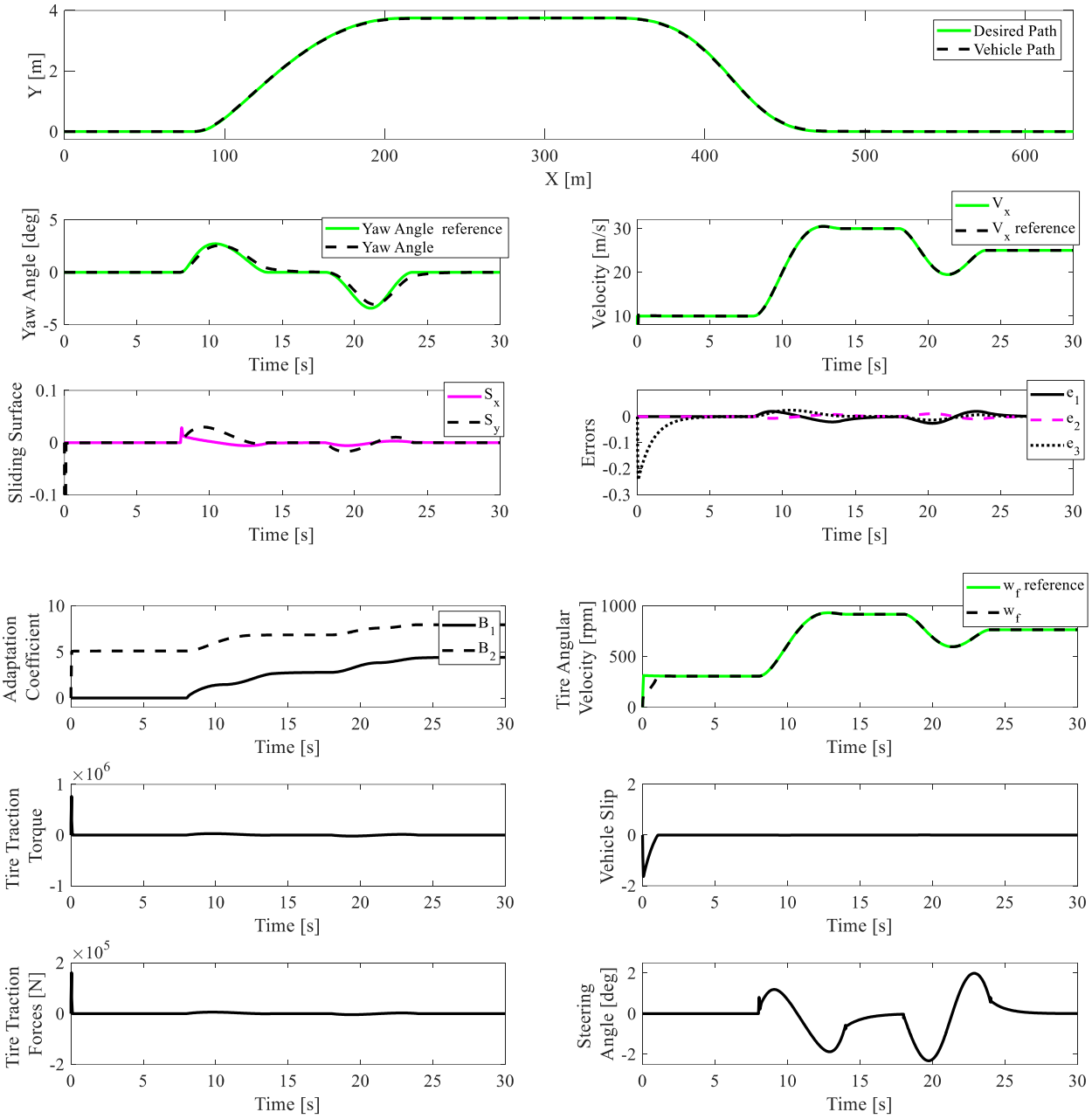

Fig. 6: The simulation results for double lane change ($\mu = 0.85$).

Conclusion

In this paper, an adaptive sliding mode control has been adopted to control the longitudinal and lateral motion of vehicle for tracking the desired trajectory in double lane change (overtaking). A sliding mode control has been used to control the front wheels' longitudinal slip, which resulted in accurate tracking and eliminating the tire longitudinal slip. Also, the proposed controller has less error in comparison with the MPC with APT. According to the simulation of the proposed control in dry and wet roads, it is concluded that the control method is capable to deal with

predefined uncertainties. Also, it is able to apply appropriate inputs to the steering angle, the angular velocity of the wheel, and the wheel's torque (some systems cannot take some parameters as inputs via actuators). Real-time tests for the proposed controller is considered as future works.

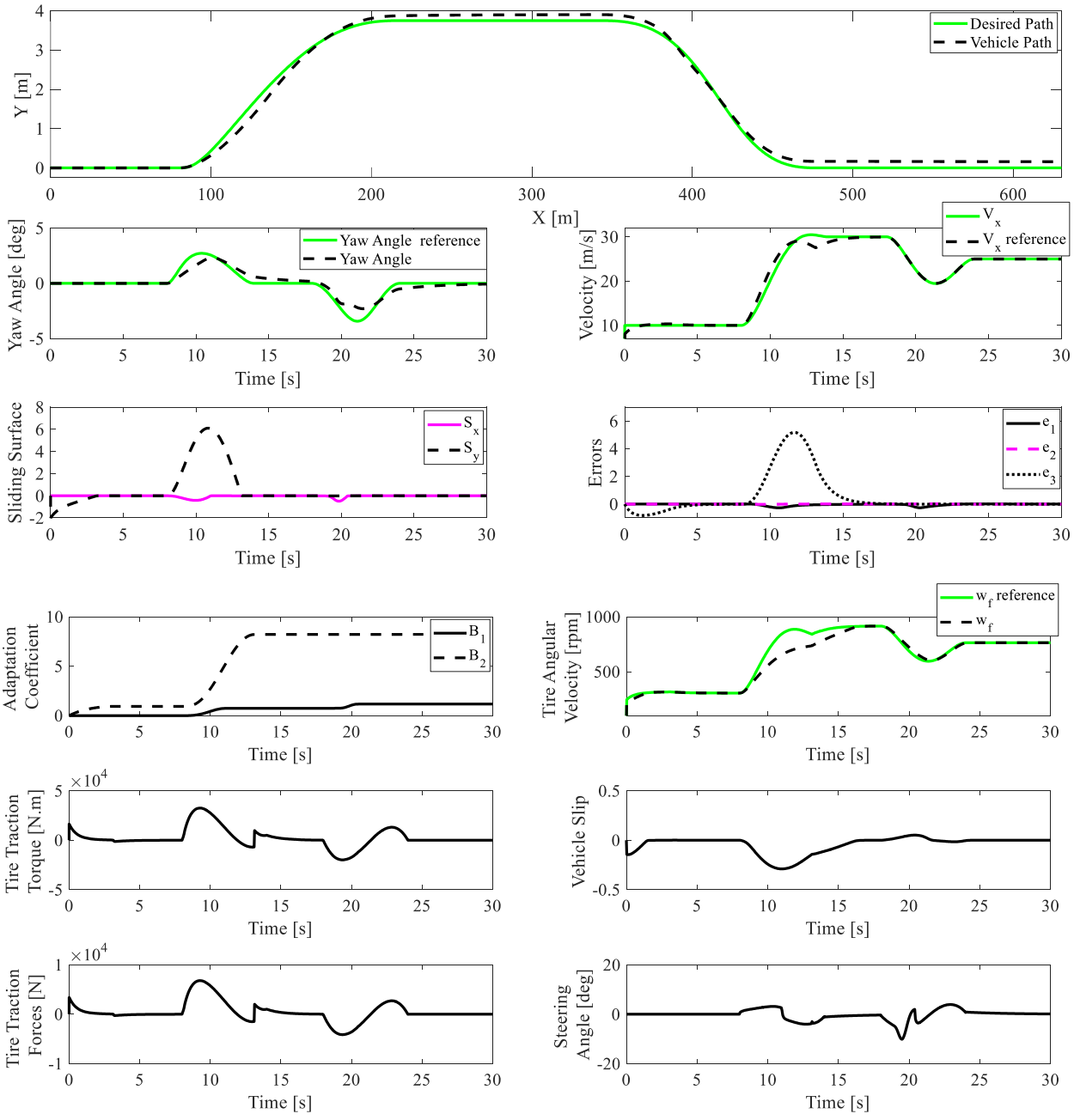

Fig. 6: The simulation results for double lane change ($\mu = 0.3$).

References

1. Urmson C, Anhalt J, Bagnell D, et al. Autonomous driving in urban environments: Boss and the urban challenge. *Journal of Field Robotics* 2008; 25: 425-466.
2. Committee SO-RAVS. Taxonomy and definitions for terms related to on-road motor vehicle automated driving systems. *SAE International* 2014.
3. AUTOMATED DRIVING SYSTEMS 2.0: A VISION FOR SAFETY - online: https://www.nhtsa.gov/sites/nhtsa.dot.gov/files/documents/13069a-ads2.0_090617_v9a_tag.pdf. *NHTSA (National Highway Traffic Safety Administration)* 2017.
4. Wu J, Liu Y, Wang F, et al. Vehicle active steering control research based on two-DOF robust internal model control. *Chinese Journal of Mechanical Engineering* 2016; 29: 739-746.
5. Poussot-Vassal C, Sename O, Dugard L, et al. Attitude and handling improvements through gain-scheduled suspensions and brakes control. *Control Engineering Practice* 2011; 19: 252-263.
6. Saikia A and Mahanta C. Vehicle stability enhancement using sliding mode based active front steering and direct yaw moment control. In: *Control Conference (ICC), 2017 Indian* 2017, pp.378-384. IEEE.
7. Klier W, Reimann G and Reinelt W. *Concept and functionality of the active front steering system*. 2004. SAE Technical Paper.
8. Li H-Z, Li L, He L, et al. PID plus fuzzy logic method for torque control in traction control system. *International Journal of Automotive Technology* 2012; 13: 441-450.
9. Li L, Ran X, Wu K, et al. A novel fuzzy logic correctional algorithm for traction control systems on uneven low-friction road conditions. *Vehicle System Dynamics* 2015; 53: 711-733.
10. Li L, Jia G, Chen J, et al. A novel vehicle dynamics stability control algorithm based on the hierarchical strategy with constrain of nonlinear tyre forces. *Vehicle system dynamics* 2015; 53: 1093-1116.
11. Norouzi A, Masoumi M, Barari A, et al. Lateral control of an autonomous vehicle using integrated backstepping and sliding mode controller. 0: 1464419318797051. DOI: 10.1177/1464419318797051.
12. Borrelli F, Falcone P, Keviczky T, et al. MPC-based approach to active steering for autonomous vehicle systems. *International Journal of Vehicle Autonomous Systems* 2005; 3: 265-291.
13. Bianchi D, Borri A, Di Benedetto MD, et al. Adaptive integrated vehicle control using active front steering and rear torque vectoring. *International Journal of Vehicle Autonomous Systems* 2010; 8: 85-105.
14. Hu C, Jing H, Wang R, et al. Robust H∞ output-feedback control for path following of autonomous ground vehicles. *Mechanical Systems and Signal Processing* 2016; 70: 414-427.
15. Canale M and Fagiano L. Stability control of 4WS vehicles using robust IMC techniques. *Vehicle System Dynamics* 2008; 46: 991-1011.
16. Norouzi A, Kazemi R and Azadi S. Vehicle lateral control in the presence of uncertainty for lane change maneuver using adaptive sliding mode control with fuzzy boundary layer. *Proceedings of the Institution of Mechanical Engineers, Part I: Journal of Systems and Control Engineering* 2018; 232: 12-28.
17. Yoshida M, Nonaka K and Sekiguchi K. Model predictive vehicle control with side slip angle restriction with suppression of modeling error by sliding mode control. In: *Control Applications (CCA), 2014 IEEE Conference on* 2014, pp.328-333. IEEE.
18. Chen B-C, Tsai C-T and Lee K. Path-Following Steering Controller of Automated Lane Change System with Adaptive Preview Time. In: *Systems, Man, and Cybernetics (SMC), 2015 IEEE International Conference on* 2015, pp.2522-2526. IEEE.
19. You F, Zhang R, Lie G, et al. Trajectory planning and tracking control for autonomous lane change maneuver based on the cooperative vehicle infrastructure system. *Expert Systems with Applications* 2015; 42: 5932-5946.

20. Rajamani R. *Vehicle dynamics and control*. Springer Science & Business Media, 2011.
21. Ackermann J. *Robust control: Systems with uncertain physical parameters*. Springer Science & Business Media, 2012.
22. Khalil HK. Noninear systems. *Prentice-Hall, New Jersey* 1996; 2: 5-1.
23. Singh KB, Arat MA and Taheri S. An intelligent tire based tire-road friction estimation technique and adaptive wheel slip controller for antilock brake system. *Journal of Dynamic Systems, Measurement, and Control* 2013; 135: 031002.

Appendix 1

Table 1. The vehicle parameters in this study

Symbol	**Description**	**quantity**
m	Mass	1704.7 [kg]
I_z	Yaw moment of inertia	3048.1 [kg.m^2]
I_ω	Wheel moment of inertia	2.6384 [kg.m^2]
l_f	Front axle-COG distance	1.025 [m]
l_r	Rear axle-COG distance	1.655 [m]
r_{eff}	Effective tire radius	0.3126 [m]
$C_{\alpha f}$	Cornering stiffness of front tire	56850 [N/rad]
$C_{\alpha r}$	Cornering stiffness of rear tire	46030 [N/rad]
μ	Tire-road friction coefficient	[0.1-0.85]
T_{df}	Wheel's torque during acceleration	
T_{bf}	Wheel's torque during braking	
C_σ	Longitudinal tire stiffness	
V_x	Actual longitudinal velocity at the axle of the wheel	
σ_x	Longitudinal slip ratio	
α	Side slip angle	
F_z	Vertical force on the tire	
F_{yf}	Lateral tire force at the front tires	
F_{yr}	Lateral tire force at the rear tires	
F_{xf}	Longitudinal tire force at the front tires	
F_{xr}	Longitudinal tire force at the rear tires	
α_f	Lateral slip angle for front wheels	
α_r	Lateral slip angle for rear wheels	
ω_w	Rotational velocity of the wheel	
δ	Front wheel steering angle	
$\dot{\psi}_{reff}$	Desired yaw rate from road	
e_1	Lateral position error with respect to road	
e_2	Yaw angle error with respect to road	
d_s	Longitudinal distance from c.g to sensor measurement point	
$\tilde{\beta}$	Switching gain	
Γ	Constant Value	
η	Constant Value	

k	Gain of the controller	
ϕ	Boundary layer	

Appendix 2

In order to prove the stability of the sliding mode control, the coefficient of switching surface can be obtained as follows [22]:

$$k_x \geq \Gamma_x\left(\bar{F}_x + \eta_x + (\Gamma_x - 1)\right)\left|\hat{F}_x\right|$$
$$k_y \geq \Gamma_y\left(\bar{F}_y + \eta_y\right) + \left(\Gamma_y - 1\right)\left|\hat{\delta}\right|$$

where,

$$\bar{F}_x = \bar{F}_1$$

$$\bar{F}_y = \bar{F}_2 + \bar{F}_1 e_2 + \bar{G}_1 F_x e_2 + d\bar{F}_3$$

And the upper and lower bounds of uncertainties for controller design are:

$$F_i^+ = F_i|_{\mu=\mu_{\max}} \qquad \hat{F}_i = \frac{F_i^+ + F_i^-}{2} \qquad \Gamma_x = \sqrt{\frac{b_x^+}{b_x^-}} = \sqrt{\frac{\mu_{\max}}{\mu_{\min}}}$$

$$F_i^- = F_i|_{\mu=\mu_{\min}} \qquad \hat{G}_i = \sqrt{G_i^+ G_i^-}$$

$$G_i^+ = G_i|_{\mu=\mu_{\max}} \qquad \bar{G}_i = \hat{G}_i - G_i^- \qquad \Gamma_y = \sqrt{\frac{b_y^+}{b_y^-}} = \sqrt{\frac{\mu_{\max}}{\mu_{\min}}}$$

$$G_i^- = G_i|_{\mu=\mu_{\min}} \qquad \bar{F}_i = \hat{F}_i - F_i^-$$

$$\mathrm{I} = 1, 2, 3, 4 \qquad \Gamma_s = \sqrt{\frac{b_s^+}{b_s^-}} = 1$$

Appendix 3

In order to prove the stability of the proposed controller, the candidate Lyapunov function has been chosen as:

$$V_x = \frac{1}{2}S_x^2 + \frac{b\hat{b}_x^{-1}}{2}\tilde{B}_x^2$$

where,

$$\tilde{B}_x = B_1 - k_x$$
$$\hat{b}_x = \hat{G}_1$$

In order to evaluate the Lyapunov function, the Lyapunov candidate function has been derived as:

$$\dot{V}_x = S_x\{F_1 + G_1F_x - \ddot{x}_{ref} + \lambda_1\dot{x} - \lambda_1\dot{x}_{ref}\} + b_x\hat{b}_x^{-1}(B_1 - k_x)\gamma_x|S_x(t)|$$

$$\dot{V}_x = S_x\{F_1 - \ddot{x}_{ref} + \lambda\dot{x} - \lambda_1\dot{x}_{ref} + b_xb_x^{-1}(-\hat{F}_1 + \ddot{x}_{ref} - \lambda_1\dot{x} + \lambda_1\dot{x}_{ref} - B_1\gamma_x tgh(S_x/\phi_x))\} + b_x\hat{b}_x^{-1}(B_1 - k_x)\gamma_x|S_x(t)|$$

According to Appendix 2,

$$\dot{V}_x \le |\bar{F}_x||S_x(t)| + \left|1 - b_x\hat{b}_x^{-1}\right|\left|\hat{F}_x\right||S_x(t)| - b_xb_x^{-1}B_1\gamma_x|S_x(t)| + b_x\hat{b}_x^{-1}(B_1 - k_x)\gamma_x|S_x(t)|$$

$$\dot{V}_x \le \bar{F}_x|S_x(t)| + \left|1 - \Gamma_y^{-1}\right|\left|\hat{F}_x\right||S_x(t)| - \Gamma_x^{-1}\left(\Gamma_x\left(\hat{F}_x + \eta_x\right) + (\Gamma_x - 1)\left|\hat{F}_x\right|\right)\gamma_x|S(t)|$$

Since η_y is a positive constant, the derivative of the Lyapunov function becomes negative only if γ_x is greater than 1, therefore:

$$\gamma_x \ge 1 \quad \rightarrow \quad \dot{V}_x \le 0$$

Hence, by choosing γ_x greater than or equal to 1, we can guarantee the system's stability based on the Lyapunov stability.

Appendix 4

In order to prove the stability of the proposed controller, the candidate Lyapunov function has been chosen as:

$$V_y = \frac{1}{2}S_y^2 + \frac{b_y\hat{b}_y^{-1}}{2}\tilde{B}_y^2$$

where,

$$\tilde{B}_y = B_2 - k_y$$
$$b_y = \hat{G}_2 + d\hat{G}_3$$

In order to evaluate the Lyapunov function, the Lyapunov candidate function has been derived as:

$$\dot{V}_y = S_y\dot{S}_y + b_y\hat{b}_y^{1-}\tilde{B}_y\dot{\tilde{B}}_y$$

$$\dot{V}_y = S_y\{F_2 + G_2\delta + (F_1 + G_1F_x)e_2 + \dot{x}\dot{e}_2 + dF_3 + dG_3\delta\} + b_y\hat{b}_y^{-1}\left(B_2 - k_y\right)\gamma_y\left|s_y\right|$$

According to Appendix 2,

$$\dot{V}_y \le \left|\bar{F}_y\right|\left|S_y(t)\right| + \left|1 - b_yb_y^{-1}\right|\left|\hat{\delta}\right|\left|S_y(t)\right| - b_yb_y^{-1}B_2\gamma_y\left|S_y(t)\right| + b_y\hat{b}_y^{-1}\left(B_2 - k_y\right)\gamma_y\left|S_y(t)\right|$$

$$\dot{V}_y \le \bar{F}_y\left|S_y(t)\right| + \left|1 - \Gamma_y^{-1}\right|\left|\hat{\delta}\right|\left|S_y(t)\right| - \Gamma_y^{-1}\left(\Gamma_y\left(\bar{F}_y + \eta_y\right) + \left(\Gamma_y - 1\right)\left|\hat{\delta}\right|\right)\gamma_y|S(t)|$$

$$\dot{V}_y \le \left(1 - \gamma_y\right)\left(F + \left|1 - \Gamma_y^{-1}\right|\left|\hat{\delta}\right|\right)\left|S_y(t)\right| - \eta_y\Gamma_y\left|S_y(t)\right|$$

Since η_y is a positive constant, the derivative of the Lyapunov function becomes negative only if γ_y is greater than 1, therefore:

$$\gamma_y \ge 1 \quad \rightarrow \quad \dot{V}_y \le 0$$

Hence, by choosing γ_y greater than or equal to 1, we can guarantee the system's stability based on the Lyapunov stability.